Electrochemistry

The Electrochemical Society of Japan

Received: June 29, 2012
Accepted: July 31, 2012
Published: October 5, 2012

http://dx.doi.org/10.5796/electrochemistry.80.700
JOI:DN/JST.JSTAGE/electrochemistry/80.700

Headline *Electrochemistry*, **80(10)**, 700–705 (2012)

# Secondary Battery Science: At the Confluence of Electrochemistry and Materials Engineering

**Esther S. TAKEUCHI,[a,b,*] Amy C. MARSCHILOK,[a,b,*] and Kenneth J. TAKEUCHI[a,*]**

[a] *Department of Chemistry, Stony Brook University, Stony Brook, NY 11794*
[b] *Department of Materials Science and Engineering, Stony Brook University, Stony Brook, NY 11794*

* *Corresponding authors: esther.takeuchi@stonybrook.edu, amy.marschilok@stonybrook.edu, kenneth.takeuchi.1@stonybrook.edu*

**ABSTRACT**

Considerations of energy density, power, and calendar life are critical to effectively develop advanced secondary systems. For next generation battery applications requiring multiple features including long life, large cycle count, high energy density and high power, new strategies are needed for the rational design of electroactive materials and electrodes. This article discusses several conceptual approaches under exploration with examples from our research group. The first approach is the systematic synthesis of materials with structures facilitating ion insertion and deinsertion at high voltage and energy density, where we control materials properties such as surface area, particle size and in particular crystallite size. A second approach is the investigation of novel electrode structures and substrates to increase energy density and capacity retention under cycling, where we have developed strategies for minimizing passive components. A third approach is investigation of catalysts for metal air batteries where the cathode active material is drawn from the air rather than carried in the battery.

© The Electrochemical Society of Japan, All rights reserved.

Keywords : Battery, Energy Density, Power, Cathode

## 1. Introduction

The advancement of battery systems with high energy and power densities remains a lynch pin for new generations of energy storage. The full utilization of renewable energy sources such as wind, photovoltaic, hydroelectric, and geothermal power depends on the ability to store energy as in many cases the renewable energy is generated on an intermittent basis. Additionally, portable electronics, hybrid vehicles, electric vehicles, biomedical devices,[1] and aerospace applications demand advanced secondary batteries that can perform safely over many years. To satisfy the needs for stationary as well as portable power, the need for improved electroactive materials and systems delivering high efficiencies when deployed for electrochemical energy storage remains acute.

The successful design of systems for rechargeable batteries involves many parameters and demands factors beyond only cycle life. Considerations of energy density, power, and calendar life are critical to effectively develop advanced secondary systems. For next generation battery applications requiring multiple features including long life, large cycle count, high energy density and high power, new strategies are needed for the rational design of electroactive materials and electrodes. This article will discuss several conceptual approaches under exploration with examples from our research group. The first approach is the systematic synthesis of materials with structures facilitating ion insertion and deinsertion at high voltage and energy density,[2–11] where we control materials properties such as surface area, particle size and in particular crystallite size. A second approach is the investigation of novel electrode structures and substrates to increase energy density and capacity retention under cycling,[12–14] where we have developed strategies for reduction of passive components. A third approach is metal air batteries where the cathode active material is drawn from the air rather than carried in the battery. We have developed and

**Esther S. TAKEUCHI** is a SUNY Distinguished Professor in the Departments of Chemistry and Materials Science and Engineering at Stony Brook University. Dr. Takeuchi received a bachelor's degree from the University of Pennsylvania with a double major in chemistry and history and completed a Ph.D. in chemistry at the Ohio State University. She completed post-doctoral work at the University of North Carolina and University at Buffalo. Dr. Takeuchi was employed previously at Greatbatch, Inc., where her achievements in lithium battery research, particularly on cells for implantable applications, led to a number of key technological developments, including the lithium/silver vanadium oxide (Li/SVO) battery, which powers the majority of implantable cardiac defibrillators (ICDs). A prolific inventor, she holds over 150 patents. She has extensively served the Electrochemical Society, most recently as President from 2011–2012. Professor Takeuchi is a member of National Academy of Engineering and has received numerous awards for her research, including an inaugural Astellas USA Foundation Award administered by the American Chemical Society for scientific work impacting public health. In 2009, Dr. Takeuchi was awarded the National Medal of Technology and Innovation by President Obama. In 2011, she was inducted into the National Inventors Hall of Fame. Her research focus is novel power sources including development of new materials and investigation of faradaic and non-faradaic mechanisms relevant to battery systems.

**Amy C. MARSCHILOK** is currently a Research Associate Professor in the Departments of Materials Science and Engineering and Chemistry at the Stony Brook University. She received her B.A. in Chemistry (English Minor) and Ph.D. in Chemistry from the University at Buffalo. She was previously employed as a Senior Scientist at Greatbatch Inc., where she was recognized as a Visionary of the Year in 2006. In 2007, she received the Leadership Award, Professional Service Category from the Western New York YWCA. In 2011, she was recognized as a Woman of Distinction by the Girl Scouts of Western New York. Her research involves synthesis, characterization and electrochemical study of novel materials and systems for energy storage, including metal-air batteries.

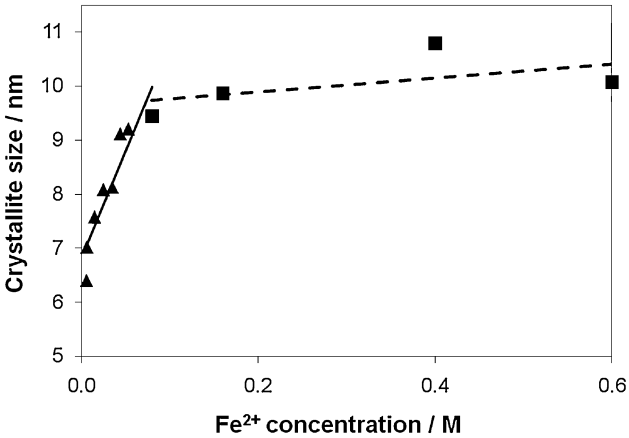


**Figure 1.** Crystallite size of $Fe_3O_4$ versus $Fe^{2+}$ reactant concentration.

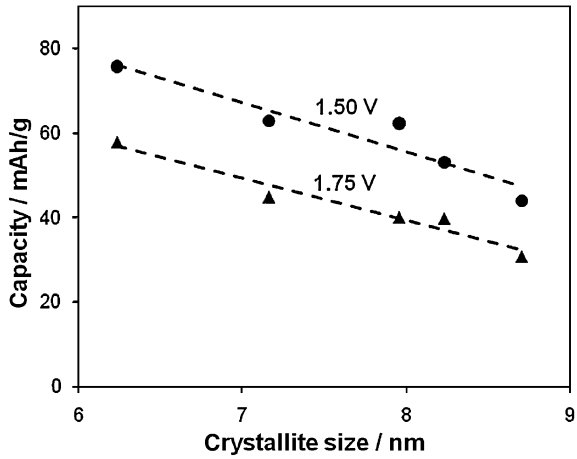


**Figure 2.** Capacity versus crystallite size for $Li/Fe_3O_4$ cells tested under 5 $mA/cm^2$ pulsatile discharge.

investigated a novel composite cathode for improved metal-air batteries.[15,16] This article is organized to discuss these three major themes and provide examples of their impact. The article is not meant to be a fully comprehensive review of the relevant literature in these research fields, but rather serves to highlight contributions in each area to illustrate their importance and potential impact.

## 2. Results and Discussion

### 2.1 Control of physical properties

Rapid ion and electron transfer are significant challenges for some classes of battery cathode materials including phosphate and oxide based materials. Based on the assumption that the charge and ion transfer associated with the electrochemical discharge process proceeds from the exterior to the interior of each active material crystallite, a size dependence of delivered capacity would be expected. Smaller crystallite size solids have a greater surface area to volume ratio than larger crystallite solids, and thus, they should support faster kinetics for charge transfer. The advantage of small crystallite size materials should be most evident at higher current densities. Thus, especially for applications demanding high power output, control of material properties including crystallite size can be especially useful.

Magnetite ($Fe_3O_4$) is an appealing material for energy storage as it is inexpensive and based on an earth abundant metal center. We developed a coprecipitation method for the preparation of pure nanosized magnetite, employing iron(III) chloride hexahydrate ($FeCl_3{\cdot}6H_2O$), iron(II) chloride tetrahydrate ($FeCl_2{\cdot}4H_2O$), and triethylamine ($N(CH_2CH_3)_3$) as reagents in aqueous solution. By modifying the concentration of reactants in solution, a series of $Fe_3O_4$ samples of differing crystallite size was systematically prepared, under low temperatures and in the absence of constraining media.[8,9] To rationalize our observed bifunctional correlation of $Fe^{2+}$ concentration and crystallite size (Fig. 1), we hypothesize that heterogeneous nucleation was dominant at low concentration, and homogeneous nucleation was dominant at high concentration.[9] Consistent with our expectations as discussed above, the most significant difference in $Fe_3O_4$ electrochemical behavior were observed under higher rate conditions. Specifically, under pulsatile discharge at 5 $mA/cm^2$, a 30% $Fe_3O_4$ crystallite size reduction improved discharge capacity by 40% (Fig. 2).

Silver hollandite ($Ag_xMn_8O_{16}$) can be described as a 1-D tunnel consisting of double chains of edge-sharing $MnO_6$ octahedra. Due to the tunneled structure of the $MnO_2$ framework, we anticipated that silver hollandite would function well as a secondary battery material as it would provide structural integrity during ion insertion and deinsertion. Silver hollandite has been difficult to prepare pure, however, we successfully developed a reflux based synthesis method for the preparation of pure silver hollandite, using silver permanganate ($AgMnO_4$), manganese sulfate ($MnSO_4$) and nitric acid ($HNO_3$) as reactants in aqueous solution. This scalable synthesis enabled the first electrochemical assessment of silver hollandite, where we observed a discharge capacity of 180 mAh/g, with good capacity retention on multiple discharge-charge cycling.[17] Refinement of the synthesis methodology enabled control of silver hollandite crystallite size, where samples ranging from nanorods ~20 nm wide (Fig. 3A) and nanorods ~10 nm wide (Fig. 3B) could be prepared.[18] Cyclic voltammetry data were collected for two samples of $Ag_xMn_8O_{16}$ with corresponding crystallite sizes of 25.6 and 12.1 nm, respectively (Fig. 4). For both the small crystallite size material and the large crystallite size material, one anodic peak and one cathodic peak were observed on each cycle. The silver hollandite with smaller crystallite size displayed more closely spaced anodic and cathodic peak voltages than the larger crystallite sized sample, illustrating a higher level of electrochemical reversibility. The peak current per gram was also higher for the small crystallite size material. Based on these preliminary results, we predict an improved ability to deliver high current with greater cycling efficiency for the smaller crystallite size silver hollandite material.

We identified silver vanadium phosphorous oxides to be a promising new family of cathode material for lithium based

**Kenneth J. TAKEUCHI** is a SUNY Distinguished Teaching Professor in the Department of Chemistry at Stony Brook University. Professor Takeuchi holds a bachelor's degree in chemistry from the University of Cincinnati and a doctorate in chemistry from The Ohio State University. In 2011, he was named a Fellow of the American Chemical Society (ACS). In addition to his research efforts, Professor Takeuchi has received over 20 awards for excellence in teaching and mentoring undergraduate and graduate students. He was named the New York state recipient of the Carnegie Foundation Professor of the Year award in 2010, and in 2008 was runner-up for the National Inspire Integrity Award from the National Society of Collegiate Scholars. He has also been recognized with an ACS Stanley Israel Regional Award for Advancing Diversity in the Chemical Sciences, and a Responsible Care National Catalyst Award from the Chemical Manufacturers Association. Professor Takeuchi's current scientific research involves the development of synthetic strategies yielding control and variation of both crystallite size on the nanometer scale and non-stoichiometric chemical composition of inorganic materials, and the subsequent utility of these inorganic materials towards energy storage.

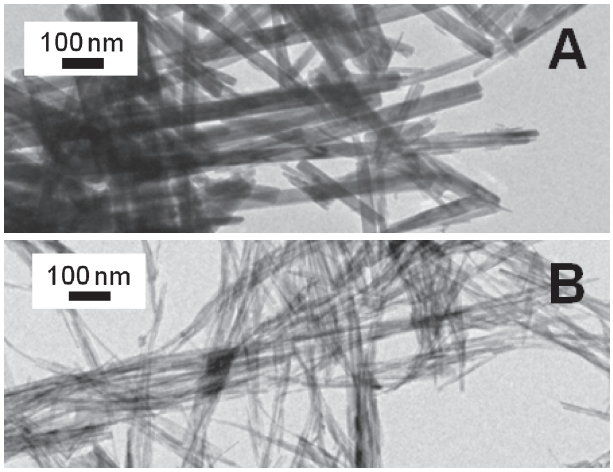


**Figure 3.** Transmission electron microscope images of silver hollandite ($Ag_xMn_8O_{16}$), 10 kX magnification for x = A) 1.46; B) 1.10.

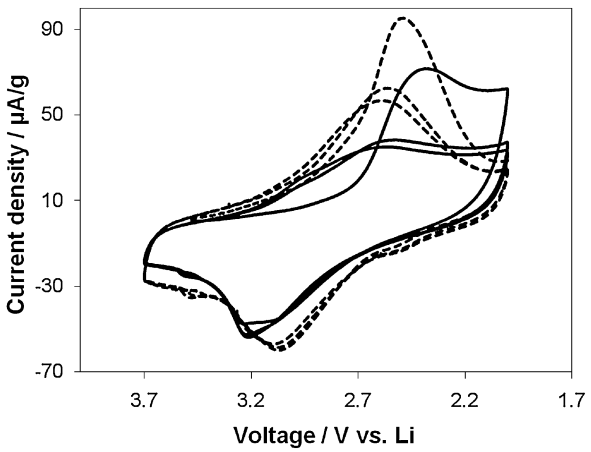


**Figure 4.** Cyclic voltammetry of $Ag_xMn_8O_{16}$ versus Li metal, for $Ag_xMn_8O_{16}$ samples with crystallite sizes of 25.6 nm (solid line) and 12.1 nm (dotted line).

batteries, in particular for high power biomedical applications such as the implantable cardiac defibrillator, based on their silver and vanadium bimetallic content.[5,19,20] Consistent with our hypothesis based on the discharge mechanism of silver vanadium oxide ($Ag_2V_4O_{11}$), as electrochemical reduction of silver vanadium phosphorous oxide ($Ag_2VO_2PO_4$, SVPO) was initiated, in-situ formation of silver nanoparticles in the cathode matrix was observed with an accompanying 15,000 fold increase in cathode conductivity.[3] The first reported preparation of $Ag_2VO_2PO_4$ employed a hydrothermal synthesis method (SVPO-H).[21] As an adaptation of our reflux synthesis method for the preparation of silver hollandite, we developed a novel ambient pressure synthesis for the preparation of SVPO (SVPO-AP), resulting in a 25% crystallite size reduction relative to the SVPO-H material.[6] Under constant current discharge, if a lower discharge rate was used (C/50 and below), the test cells with SVPO-AP and SVPO-H showed similar voltages and delivered similar total capacities. At the highest discharge rate used (C/10) the cells using SVPO-AP showed higher middle of life voltages, but no increases in delivered capacities. To investigate cell behavior under conditions more consistent with a high power biomedical application such as the ICD, test cells were discharged with intermittent pulses at alternating current densities. Resistance at each pulse was calculated using Ohm's law and cells containing SVPO-AP showed lower resistances. Interestingly, differences in the ohmic resistances of the SVPO materials were more significant than differences in the polarization resistance, where a representative example for one pulse

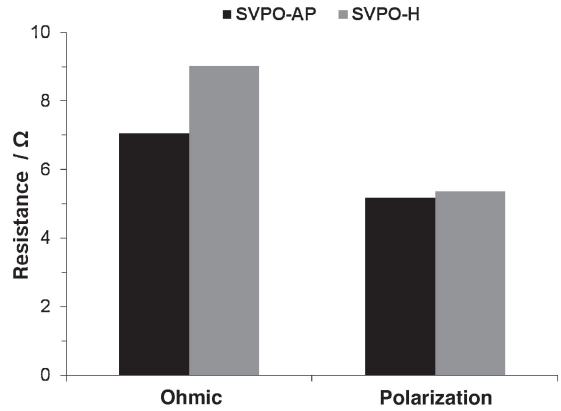


**Figure 5.** Ohmic and polarization contribution to cell resistance of Li/SVPO-AP and Li/SVPO-H electrochemical cells under 40 mA/cm$^2$ pulse at 100 mAh/g.

is shown (Fig. 5). Less voltage drop and lower resistance of the cells using the SVPO-AP cathodes can provide better power capability for high current load applications.

## 2.2 Alternative electrode structures and substrates

Battery electrodes are most typically prepared by combining carbon (conductive additives), polymer (binder) and active material particles into a slurry or paste which is then coated onto a metallic foil (current collector) to form a composite electrode. The three passive components within a conventional battery electrode serve distinct and important functions. However, none of the materials contribute directly to energy density, thus, it is desirable to minimize the mass of the inert materials. Additionally, conventional electrode coatings include constituents that may be electrically insulating including the polymeric binders and often the active material (Fig. 6A). Therefore, the conducting particles, often carbon based, play an important role as they must provide a percolation network throughout the body of the electrode. Since percolation occurs when a three dimensional interconnected conducting network is formed throughout a composite,[12] the challenge is to use a quantity of conductive additive adequate to develop a percolation network but to avoid the use of excessive conductive additive to minimize detrimental impacts on energy density.

Carbon nanotubes (CNT) consist of graphene sheets wrapped to form cylindrical tubes, and may be single-walled (SWCNT) or multi-walled (MWCNT). When used as additives, percolation thresholds ranging from less than 1.0 to greater than 10.0 weight % CNT have been observed experimentally depending on the type of CNT used, the polymer matrix, and processing technology.[22] It has also been observed that an insulating binder that is distinct from the conductive additive may give rise to polarization. Even thin polymer coatings can result in significant polarization, where there may be a change in the mechanism of conduction between the CNT fibers.[23] Further, structural damage to MWCNT during the dispersion process used in preparation of electrode slurries prior to electrode coating can result in diminished benefit of CNT over carbon black.[24] Thus, CNT additives may not always be used to full advantage when used in a conventional electrode. Therefore, we were interested in exploring the use of pre-formed carbon nanotube substrates, termed (CNTS), to replace the conventional conductive additives and binders.

The use of CNTS provides additional benefits in terms of the voltage window of stability. As the drive toward high energy density continues, higher voltage active materials are being explored. Aluminum foil has been most commonly used as the current collector for lithium ion battery cathodes, however, even aluminum is susceptible to corrosion with certain combinations of electrolyte

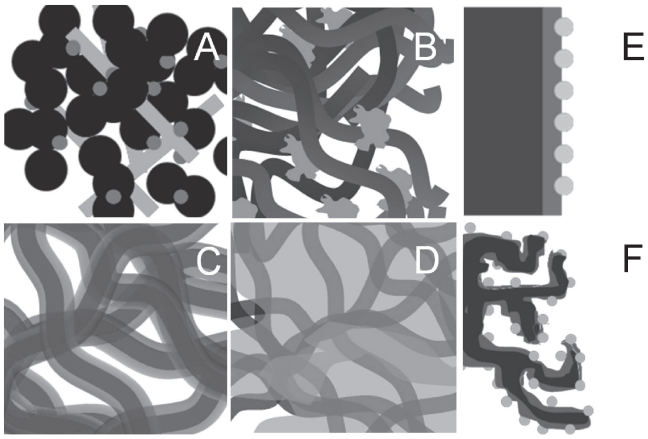


**Figure 6.** Conceptual schematic showing A) Conventional electrode coating comprised of conductive carbon (black spheres), insulating binder (grey rods), and active material (grey spheres); B) Particle deposition (PS) method composite electrode consisting of carbon nanotube substrate (black rods) with active material (grey) deposit; C) Substrate integration (SI) method composite electrode consisting of carbon nanotube substrate (black rods) with active material (grey) deposit, low active material loading; D) Substrate integration (SI) method composite electrode consisting of carbon nanotube substrate (black rods) with active material (grey) deposit, high active material loading; E) Composite air electrode consisting of planar carbon substrate (black), conductive polymer (dark grey), and catalyst (light grey spheres); F) Composite air electrode consisting of three-dimensional carbon substrate (black), conductive polymer (dark grey), and catalyst (light grey spheres).

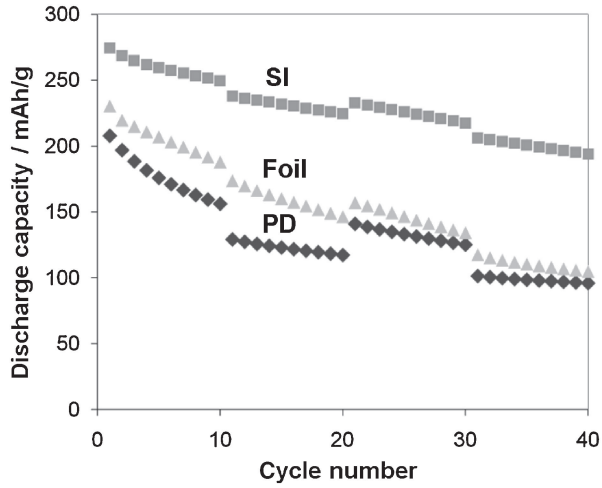


**Figure 7.** Cycle testing for $Li/V_2O_5$-CNTS based electrodes prepared using particle deposition (PD), substrate integration (SI), and foil coating methods. For cycles 1–10, 21–30, the discharge rate is C/5 and for cycles 11–20, 31–40 the discharge rate is C/2.

and high voltage cathodes.[25–27] In contrast, CNT demonstrate high oxidative stability.[28] In addition, CNTS have the needed characteristics for next generation cathode current collectors, including strength, flexibility, and ability to be fabricated in variable thicknesses and on a large scale.

Theoretical calculations were used to assess the potential advantage of CNTS as cathode current collectors, including the elimination of the aluminum foil as current collector, the inert binder and additional conductive additives. An active capacity of 270 mAh/g of active material was used for this estimate. For the conventional electrode, a composite electrode using 85% active material was assumed. A conventional electrode with an aluminum foil current collector (20 microns), the composite electrode would provide 114 mAh/g of total electrode for a single-sided coating and 152 mAh/g of total electrode for a double-sided coating per 1 sq cm of electrode. If a CNTS is substituted for the binder, carbon black and aluminum foil an active material loading of 4.5 mg/cm$^2$, 1 sq cm of electrode can provide 187 mAh/g of delivered capacity. Thus, the effective gravimetric energy density of a positive electrode may increase by 20–60% with no change in active material. As experimentally determined, the CNTS are thicker than aluminium foil and thus a direct advantage in volumetric energy density would not be anticipated when measured by conventional methods. However, since the CNTS are porous, a significant part of the volumetric disadvantage may be offset due to the elimination of binder and other conductive additives.

Our research group has developed two methods to prepare electrodes using the carbon nanotube substrates (CNTS).[12–14] One method involved the isolation and deposition of active particles on a preformed CNTS, this was termed PD or particle deposition (Fig. 6B). A second method was used with a more direct integration of the active material using a novel substrate integration or SI method (Figs. 6C and 6D). This method entailed introduction of the CNTS to the active material during a sol gel process without prior isolation of the active material. Notably, in both cases the prepared CNTS electrodes contained no polymeric binder or additional conductive additive beyond the CNTS.

The electrochemical behavior of the cathodes was investigated. The electrodes explored were vanadium oxide active material ($V_2O_5$) deposited on CNTS using the PD method, electrodes prepared by the SI method, and electrodes prepared by the conventional method using coatings on aluminum foil (Fig. 7).[13] Discharge curves tested at C/5 showed similar delivered capacities for the PD method and the coated aluminum foil method at 206 and 218 mAh/g, respectively. In contrast, the delivered capacities of the SI prepared electrodes were the highest, at 270 mAh/g. Capacity retention during cycle life was also assessed as a function of electrode type. Testing was conducted by applying 40 discharge-charge cycles, using a C/5 discharge rate for cycles 1–10, 21–30, and a C/2 discharge rate for cycles 11–20, 31–40. The highest capacity retention was observed for the SI electrodes compared to the electrodes prepared by PD and conventional coated foil electrodes.

Due to the differences in the deposition method, the integration of the active material of the SI electrodes is more complete relative to the material prepared by the PD method. The capacity dependence on weight per unit area was investigated in more detail where cells were prepared using the PD and SI electrode with a range of different active material loadings were cycled under different discharge rates. Both PD and SI electrodes showed a general trend of somewhat decreasing delivered capacity per gram of active material with increasing mass loading. Under higher rate (C/2) discharge, the SI method showed significantly higher delivered capacities.

The approach used to prepare CNTS-$M_xO_y$ composite electrodes has also been extended to other materials where $LiV_3O_8$ based cathodes were prepared.[14] Carbon nanotube substrates (CNTS) incorporated with lithium trivanadate ($LiV_3O_8$) synthesized from a sol-gel method were heat treated prior to electrochemical characterization. Testing using a galvanostatic discharge-charge type approach was done versus lithium metal anodes. During the electrochemical reduction of $Li_{1+x}V_3O_8$, the polarization was higher in the region of $x = 0.5$, then lower in the region $0.5 < x \leq 1.6$, and increased again at states of discharge ($x > 1.6$). These results are reminiscent of previous reports which have indicated higher levels of polarization where $x = 1.5$ or 2.0.[29–31]

Test cells using the CNTS-$LiV_3O_8$ cathodes were discharged at a current rates equal to C/20 to the desired voltage of 2.0, 2.4, or 2.5 V and then charged at a current rate equal to C/10 to 3.7 V. Subsequent to the initial discharge curve, the test cells were charged to 3.8 V at a current rate equal to C/10, held at the high potential for 2 h, and then discharged at a rate of C/5. The cells were tested in this manner for 100 discharge-charge cycles. The capacities delivered by the cells discharged to 2.0 V were 280 mAh/g of active material, while the cells discharged to 2.4 and 2.5 V delivered capacities of 210 and 160 mAh/g, respectively. When the cells reached cycle 100, all groups were providing discharge capacities > 130 mAh/g and discharge energies > 390 mWh/g. The capacity fade was lower for the cells discharged to 2.4 and 2.5 V compared to the cells discharged to 2.0 V. The cells discharged to 2.4 and 2.5 V start to outperform the cells discharged to 2.0 V cell by about the 80th cycle. If specific energy is considered, the 2.4 and 2.5 V cells begin to outperform the 2.0 V cells by the 70th cycle due to their higher average loaded voltage. Thus, cells discharged to 2.4 and 2.5 V delivered improved capacity retention relative to the cells discharged to 2.0 V. The capacity retention for the cells as a percentages of first cycle capacity for cycle 100 were 51, 79, and 86% under the 2.0, 2.4, and 2.5 V limits, respectively. These results demonstrate that the CNTS method was effectively translated to an additional chemical cathode system. In this case, a 36% mass savings is achieved by the CNTS electrode when the total electrode mass is considered for the foil composite electrode versus the CNTS electrode. These results affirm the opportunity for cell level energy density improvement based on the electrode fabrication method using CNTS electrodes.

### 2.3 Metal air cathodes

In conventional batteries, the electroactive materials are placed inside the battery housing as part of the battery manufacturing process. A desirable solution for next generation energy storage may be metal air batteries. The electroactive cathode material in metal air batteries (oxygen) is captured from ambient air and thus, is not an initial part of the battery structure. Thus, even when the mass gained during discharge due to formation of oxygen reduction products is considered,[15,16] metal air batteries offer the opportunity for significant energy density increases when compared to conventional battery technologies.

Since oxygen is the electroactive cathode material in a metal air battery, all solid structural components on the positive end of the battery are "passive" and traditional classifications of active material do not apply. Although the specific chemistry of the physical structure residing at the cathode (the "air electrode") can be varied, it must be structurally sound, conductive, and effectively catalyze the oxygen reduction reaction. Typically, a composite comprising a conductive material physically mixed with an oxygen reduction catalyst is utilized, often integrated with binder[10,11] and a metal mesh as support.[32,33] Thus, the conventional approach to air electrodes positions catalyst particles randomly throughout the thickness of the composite electrode, analogous to the positioning of active material particles within a conventional battery electrode (Fig. 6A). A disadvantage of the conventional air electrode fabrication strategy is that catalyst particles positioned within the electrode interior will have limited access to oxygen.

We recently reported a new design strategy for the preparation of air electrodes. Using electrodeposition methods, a planar three-component composite electrode consisting of a carbon (C) current collector substrate was successively coated with a conductive polymer (cp) layer and a silver (Ag) nanoparticle coating. Counter to conventional air electrode fabrication strategies, our preparation method positioned all of the catalyst nanoparticles on the outer surface of the composite electrode, allowing facile access of oxygen gas molecules to the catalyst particle surfaces (Fig. 6E). An additional benefit of our approach is the use of a conductive polymer, in contrast to the insulating polymers used in conventional air electrodes.

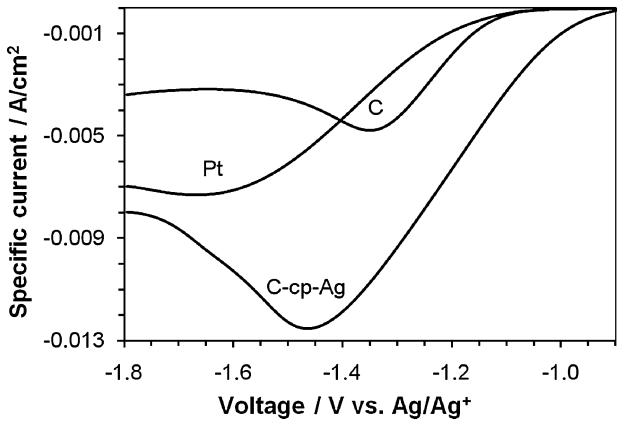


**Figure 8.** Oxygen reduction activity in nonaqueous oxygen saturated solution for uncoated glassy carbon (C), platinum disk (Pt), and carbon-conductive polymer-silver (C-cp-Ag) composite electrodes.

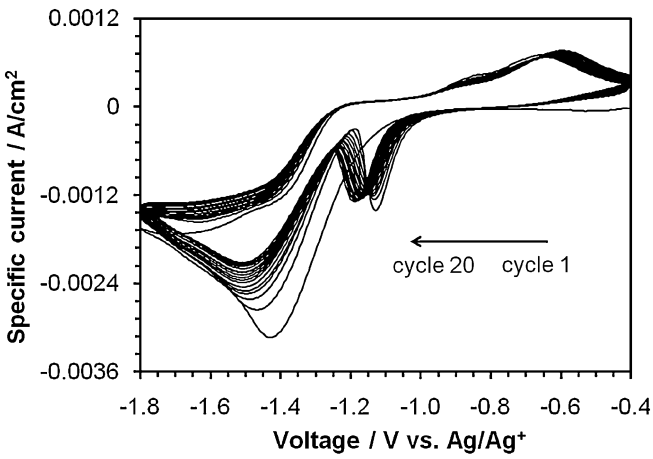


**Figure 9.** Multiple cycling of carbon-conductive polymer-silver (C-cp-Ag) composite electrode in air saturated nonaqueous solution, 20 consecutive cycles at 100 mV/s.

In nonaqueous solution, our planar C-cp-Ag composite electrodes exhibited 2X improved oxygen reduction capability relative to uncoated glassy carbon electrodes, also comparing favorably with a platinum (Pt) disk electrode (Fig. 8),[34] and showing comparable activity to a gold (Au) disk electrode.[35] AC impedance measurements taken to assess the conductivity of the C-cp-Ag composite electrode near open circuit potential and at an appropriate potential for oxygen reduction verified that the composite electrode maintained its conductivity at a negative potential appropriate for oxygen reduction. In addition, a C-cp-Ag composite electrode showed quasi-reversible oxygen reduction behavior over 20 consecutive cycles at a high scan rate of 100 mV/s (Fig. 9). This shows feasibility for possible future use of the C-cp-Ag electrode in a secondary battery application.

The roles of the substrate, conductive polymer, and catalyst were assessed in a series of experiments.[36] By varying the chemistry of the substrate, we established that the oxygen reduction activity of the composite electrode is dictated by the conductive polymer and not the underlying substrate, opening the possibility for the use of diverse types of current collector substrates for silver-polymer composite electrodes in the future. Next, an electrode durability test was designed, which showed a significant benefit of the conductive polymer in terms of activity retention. Most significantly, we were

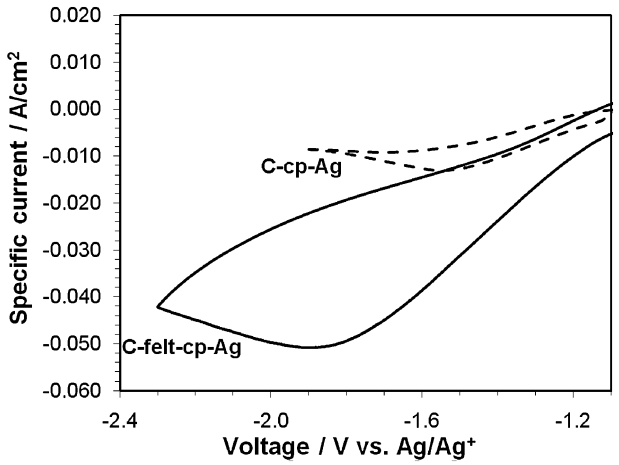


**Figure 10.** Oxygen reduction activity in oxygen saturated non-aqueous solution for planar glassy carbon-conductive polymer-silver (C-cp-Ag) and 3D carbon felt-conductive polymer-silver (Cfelt-cp-Ag) composite electrodes.

able to establish optimum C-cp-Ag composite electrode activity at a low Ag catalyst loading of 0.08 mg/cm$^2$.[16] This shows that a low cost composite electrode can be achieved using this design metholodogy.

Another advantage of our electrodeposition strategy is the ability to easily generate three-dimensionally structured composites via use of three dimensional carbon substrates (Fig. 6F). A consistent mass-charge relationship for conductive polymer deposition was established, across multiple current collector substrates ranging from low to high surface area, verifying that the conducting polymer deposition was a well controlled process which was not sensitive to the geometry of the current collector substrate. Composite electrodes utilizing carbon felt (C-felt) as substrates with conductive polymer and silver coatings were prepared and evaluated. The 3D Cfelt-cp-Ag composite exhibited ~4X enhancement in oxygen reduction activity over a planar C-cp-Ag electrode (Fig. 10). This data highlights the substantial opportunity that transitioning to a 3D architecture can provide for metal air batteries.

## 3. Summary

Three themes for next generation battery cathodes under active investigation by our research group have been described in this highlight. First, the profound impact of crystallite size control on delivered energy density and power output has been illustrated, in the context of three specific materials which represent different structures as well as compositions, magnetite ($Fe_3O_4$), silver hollandite ($Ag_xMn_8O_{16}$), and silver vanadium phosphorous oxide ($Ag_2VO_2PO_4$). Secondly, a new cathode fabrication strategy which increases energy density and improves capacity retention during cycling is accomplished via direct integration of active materials with a preformed carbon nanotube substrate. Results achieved using this methodology with two vanadium based cathode materials, $V_2O_5$ and $LiV_3O_8$, are described. Third, we have developed and investigated a novel composite cathode for metal-air batteries which utilizes an electrodeposition based fabrication methodology and a conductive polymer. This methodology is demonstrated in both two-dimensional (planar) and three dimensional geometries. Significant increases in oxygen reduction activity are achieved with the opportunity for low cost, as a silver catalyst can be utilized, with a low catalyst loading $<0.1$ mg/cm$^2$ required.

These three themes provide pathways for increased energy density, power output, and cycle life. These strategies can contribute to addressing the ever growing need for lightweight, long-life, high power energy storage solutions.

## Acknowledgment

Funding from the following sources is gratefully acknowledged: Department of Energy, Office of Basic Energy Sciences (Grant DE-SC0002460), National Institutes of Health, National Heart, Lung, and Blood Institute (Grant 1R01HL093044-01A1), the Air Force Office of Scientific Research (Award FA9550-09-1-0334), and the New York State Energy Research and Development Authority, NYSERDA (Agreement 18517).

## References

1. D. C. Bock, A. C. Marschilok, K. J. Takeuchi, and E. S. Takeuchi, (submitted for publication).
2. A. C. Marschilok, K. J. Takeuchi, and E. S. Takeuchi, *Electrochem. Solid-State Lett.*, **12**, A5 (2009).
3. E. S. Takeuchi, A. C. Marschilok, K. Tanzil, E. S. Kozarsky, S. Zhu, and K. J. Takeuchi, *Chem. Mater.*, **21**, 4934 (2009).
4. A. C. Marschilok, E. S. Kozarsky, K. Tanzil, S. Zhu, K. J. Takeuchi, and E. S. Takeuchi, *J. Power Sources*, **195**, 6839 (2010).
5. Y. J. Kim, C. Y. Lee, A. C. Marschilok, K. J. Takeuchi, and E. S. Takeuchi, *J. Power Sources*, **196**, 3325 (2011).
6. Y. J. Kim, A. C. Marschilok, K. J. Takeuchi, and E. S. Takeuchi, *J. Power Sources*, **196**, 6781 (2011).
7. K. E. Farley, A. C. Marschilok, E. S. Takeuchi, and K. J. Takeuchi, *Electrochem. Solid-State Lett.*, **15**, A1 (2011).
8. S. Zhu, A. C. Marschilok, E. S. Takeuchi, and K. J. Takeuchi, *Electrochem. Solid-State Lett.*, **12**, A91 (2009).
9. S. Zhu, A. C. Marschilok, E. S. Takeuchi, G. T. Yee, G. Wang, and K. J. Takeuchi, *J. Electrochem. Soc.*, **157**, A1158 (2010).
10. A. Debart, A. J. Paterson, J. Bao, and P. G. Bruce, *Angew. Chem., Int. Ed.*, **47**, 4521 (2008).
11. J. K. Ngala, S. Alia, A. Dobley, V. M. B. Crisostomo, and S. L. Suib, *Chem. Mater.*, **19**, 229 (2007).
12. S. Kirkpatrick, *Rev. Mod. Phys.*, **45**, 574 (1973).
13. A. Marschilok, C.-Y. Lee, A. Subramanian, K. J. Takeuchi, and E. S. Takeuchi, *Energy Environ. Sci.*, **4**, 2943 (2011).
14. C.-Y. Lee, A. C. Marschilok, A. Subramanian, K. J. Takeuchi, and E. S. Takeuchi, *Phys. Chem. Chem. Phys.*, **13**, 18047 (2011).
15. S. S. Sandhu, G. W. Brutchen, and J. P. Fellner, *J. Power Sources*, **170**, 196 (2007).
16. S. S. Sandhu, J. P. Fellner, and G. W. Brutchen, *J. Power Sources*, **164**, 365 (2007).
17. S. Zhu, A. C. Marschilok, C.-Y. Lee, E. S. Takeuchi, and K. J. Takeuchi, *Electrochem. Solid-State Lett.*, **13**, A98 (2010).
18. D. B. Le, S. Passerini, J. Guo, J. Ressler, B. B. Owens, and W. H. Smyrl, *J. Electrochem. Soc.*, **143**, 2099 (1996).
19. A. C. Marschilok, K. J. Takeuchi, and E. S. Takeuchi, *Electrochem. Solid-State Lett.*, **12**, A5 (2009).
20. A. C. Marschilok, E. S. Kozarsky, K. Tanzil, S. Zhu, K. J. Takeuchi, and E. S. Takeuchi, *J. Power Sources*, **195**, 6839 (2010).
21. H. Y. Kang, S. L. Wang, P. P. Tsai, and K. H. Lii, *J. Chem. Soc., Dalton Trans.*, 1525 (1993).
22. N. Hu, Z. Masuda, G. Yamamoto, H. Fukunaga, T. Hashida, and J. Qiu, *Composites, Part A*, **39**, 893 (2008).
23. E. Kymakis and G. A. J. Amaratunga, *J. Appl. Phys.*, **99**, 084302 (2006).
24. J.-H. Lee, G.-S. Kim, Y.-M. Choi, W. I. Park, J. A. Rogers, and U. Paik, *J. Power Sources*, **184**, 308 (2008).
25. A. Abouimrane, J. Ding, and I. J. Davidson, *J. Power Sources*, **189**, 693 (2009).
26. L. J. Krause, W. Lamanna, J. Summerfield, M. Engle, G. Korba, R. Loch, and R. Atanasoski, *J. Power Sources*, **68**, 320 (1997).
27. K. Xu, *Chem. Rev.*, **104**, 4303 (2004).
28. K. Lee, L. Zhang, H. Lui, R. Hui, Z. Shi, and J. Zhang, *Electrochim. Acta*, **54**, 4704 (2009).
29. G. Sudant, E. Baudrin, B. Dunn, and J.-M. Tarascon, *J. Electrochem. Soc.*, **151**, A666 (2004).
30. J. Livage, *Chem. Mater.*, **3**, 578 (1991).
31. F. Coustier, S. Passerini, and W. H. Smyrl, *J. Electrochem. Soc.*, **145**, L73 (1998).
32. W. Xu, J. Xiao, D. Wang, J. Zhang, and J.-G. Zhang, *J. Electrochem. Soc.*, **157**, A219 (2010).
33. W. Xu, J. Xiao, J. Zhang, D. Wang, and J.-G. Zhang, *J. Electrochem. Soc.*, **156**, A773 (2009).
34. S. H. Lee, S. Zhu, C. C. Milleville, C.-Y. Lee, P. Chen, K. J. Takeuchi, E. S. Takeuchi, and A. C. Marschilok, *Electrochem. Solid-State Lett.*, **13**, A162 (2010).
35. W. Dong, J. Sakamoto, and B. Dunn, *J. Sol-Gel Sci. Technol.*, **26**, 641 (2003).
36. A. C. Marschilok, S. Zhu, C. C. Milleville, S. H. Lee, E. S. Takeuchi, and K. J. Takeuchi, *J. Electrochem. Soc.*, **158**, A223 (2011).